

SEISMIC MICROZONATION STUDIES BY USING THE EQUIVALENT LINEAR APPROACH (L'AQUILA, CENTRAL ITALY)

M. Tallini¹, E. Morana² & V. Guerriero³

¹ Dipartimento di Ingegneria Civile, Edile-Architettura e Ambientale, Università dell'Aquila, Italy, email marco.tallini@univaq.it

² Dipartimento di Ingegneria Civile, Edile-Architettura e Ambientale, Università dell'Aquila, Italy

³ Dipartimento di Ingegneria Civile, Edile-Architettura e Ambientale, Università dell'Aquila, Italy

Abstract: This contribution is part of the third level Seismic Microzonation project activities carried out on pilot areas of L'Aquila Municipality area and financed by the Abruzzo Region (Department of Government of the Territory and Environmental Policies - Risk Prevention Service of Civil Protection). L'Aquila Municipality area pertains geologically to the middle Aterno River intermontane basin which was filled up by Plio-Quaternary coarse- and fine-grained detrital deposits related mainly to lacustrine, slope and alluvial environments. It is characterised furthermore by a notable seismic hazard as showed by the recent April 6, 2009 Mw 6.29 near source earthquake and the far field Central Italy 2016 seismic sequence. According to the Italian Civil Protection Department guidelines numerical maps and database were produced at the end of the third level Seismic Microzonation project. The project was realized through the following activities: (i) update of database concerning boreholes, geotechnical and geophysical in-situ investigations; (ii) far field and near source seismic input selection; (iii) computer code selection; (iv) geophysical and geotechnical soil characterization; (v) definition of the geological sections; (vi) 1D and 2D modelling; (vii) mapping the third level Seismic Microzonation zones based on the calculated Amplification Factors; (viii) third level Seismic Microzonation numerical maps elaboration. Considering the complex seismostratigraphy of L'Aquila Municipality area, 2D modeling was carried out on a very large number of sections to calculate in-depth the AFs and analyze their areal variation. The nonlinear soil behaviour is taken into account by performing equivalent linear simulations. The validity of 2D modelling was confirmed by the congruence between the geological background and the AFs value distribution. The 2D modelling allowed to verify the existence of basin and basin edge effects via the comparison with 1D simulations (Preturo-Sassa area). In the Bazzano-Monticchio area crossing the Aterno R. plain, the AF values increase for the intervals of the higher periods which could be possibly linked to 2D effect.

1. Introduction

The proposed study is part of the third level Seismic Microzonation (SM) project activities carried out on a 7 km² wide pilot areas (Preturo-Sassa and Bazzano-Monticchio) of L'Aquila Municipality financed by the Abruzzo Region (Department of Government of the Territory and Environmental Policies - Risk Prevention Service of Civil Protection) (Fig. 1).

L'Aquila Municipality pertains geologically to the middle Aterno River intermontane basin which was filled up by Plio-Quaternary coarse- and fine-grained detrital deposits related mainly to lacustrine, slope and alluvial environments. It is characterised furthermore by a notable seismic hazard as evidenced by the recent April 6, 2009, Mw 6.29 near source earthquake (Nocentini et al., 2017; 2018).

According to the Italian Department of Civil Protection guidelines (SM Working Group, 2008), numerical maps and database were produced at the end of the third level SM project. The project was realized through the following activities, carried out in sequence and, partly, in parallel way: (i) update of database concerning boreholes, geotechnical and geophysical in-situ investigations; (ii) seismic input selection; (iii) computer code selection; (iv) geophysical and geotechnical soil characterization; (v) definition of the geological sections; (vi) 1D and 2D modelling; (vii) the third level SM microzones based on the calculated Amplification Factors; (viii) third level SM numerical maps elaboration.

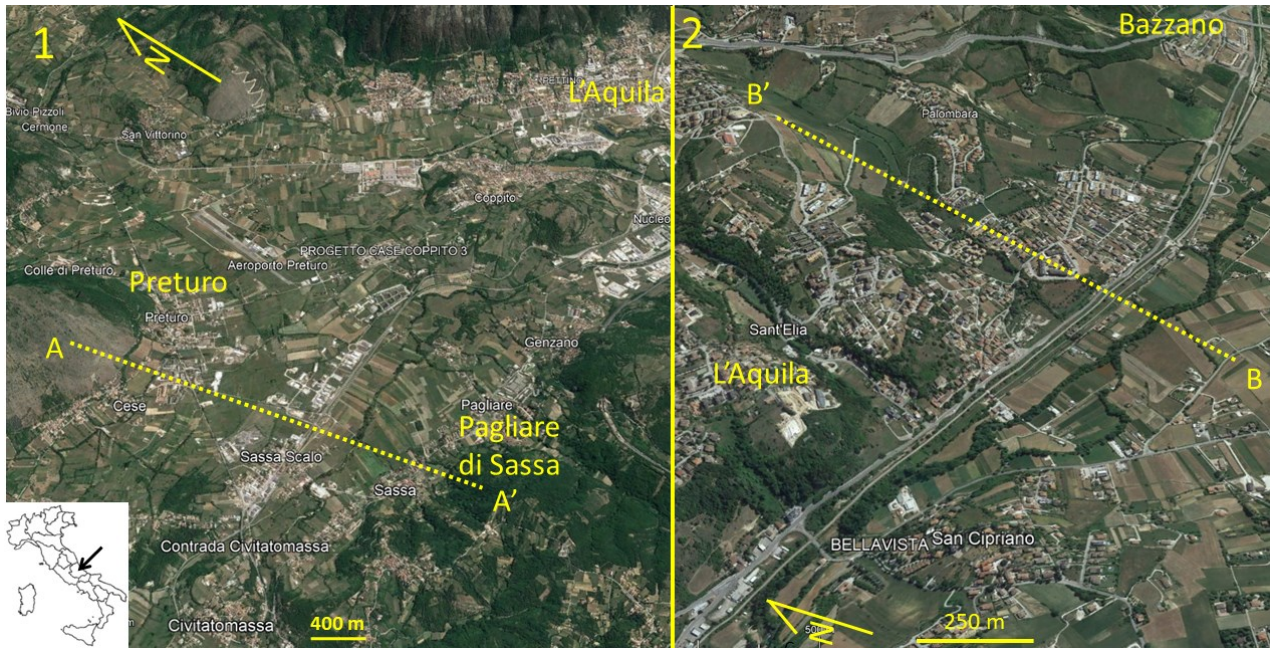


Figure 1. The study area of Preturo – Sassa (1) and Bazzano – Monticchio (2) (L'Aquila Municipality). The dotted yellow lines refer to the section A-A' and B-B'.

2. Database and seismic input

Within the third level SM project, the previous elaborated first level SM database was updated with new *ad hoc* investigations that were placed in remarkable sites of the pilot areas.

Given the complex seismostratigraphy of middle Aterno River basin, characterized by a thick and complex sedimentary sequence, four 2D seismic arrays were performed which permitted to obtain the V_s profile up to great depths reaching the Meso-Cenozoic calcareous-terrigenous substratum.

Following the Italian technical standards for construction NTC18 (CS.LL.PP., 2018), seven natural accelerograms were selected as seismic inputs and were used in the numerical simulations for the estimation of the Amplification Factors (AF). The online database used for the selection of the seven recordings is REXELite which is available at the link: https://itaca.mi.ingv.it/ItacaNet_40/#/rexel. REXELite is the simplified version of the Rexel database (Iervolino et al., 2009).

The used target response spectrum for L'Aquila town (latitude: 42.377; longitude: 13.310) is that associated with a reference earthquake with a return period of 475 years, on seismic bedrock ($V_s > 800$ m/s), horizontal topography and 5% damping.

In choosing the seven natural accelerograms, based on the target spectrum, the following characteristics of the selected seismic events and recording sites were considered (Fig. 2): (i) magnitude earthquake (M_w or M_I - interval): 5.5 – 7; (ii) focal mechanism: extensional fault; (iii) epicentral distance from the recording site: 0-30 km; (iv) recording site on seismic bedrock. Moreover, the used tolerance criteria between the target spectrum and the average value of the seven selected recordings are: (i) period range considered for comparison: 0.1-1.1 s; (ii) upper tolerance: 30 %; (iii) lower tolerance: 10 %.

Seismic input: reference spectrum versus average spectrum of 7 selected accelerograms

green: reference spectrum, normative spectrum used as target
 Red: upper tolerance
 Blue: lower tolerance
 Gray: average spectrum which has to be in between the tolerance boundaries

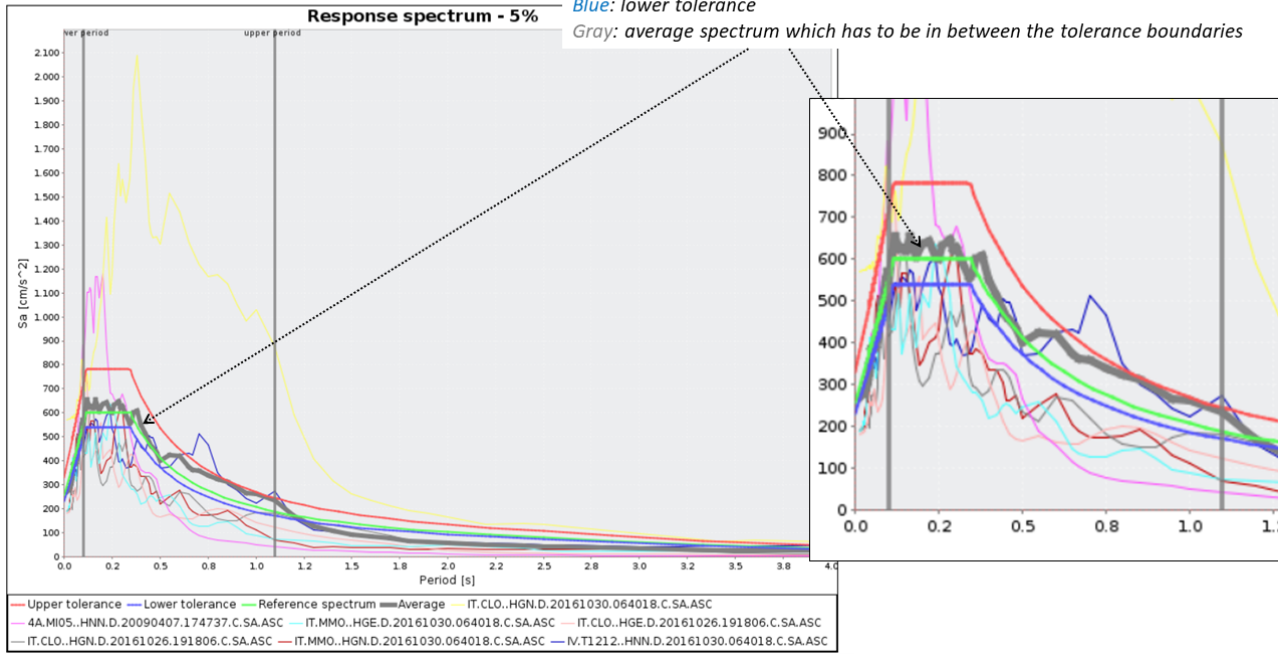


Figure 2. The seven seismic input accelerograms selected by REXELite database (Iervolino et al., 2009) for this study.

3. Computer code selection

3.1. The nonlinear behavior of real soil and the linear equivalent approach to numerical simulation

In general, when subjected to cyclic loads, soils show nonlinear behavior characterized by hysteresis cycles on the shear stress T - shear strain γ plane. In numerical analyses, the possible procedures used to take into account the nonlinear constitutive model of the soil are divided into: (i) the equivalent linear approach and (ii) the incremental nonlinear approach. The equivalent linear approach consists in executing of a series of linear analyses where the soil nonlinear behavior is described through the secant shear stiffness modulus G , given by the ratio τ/γ and the damping ratio D , which is proportional to the area of the hysteresis loop according to the relationship (1).

$$D = W_D / 4\pi W_E \tag{1}$$

where: D is the damping ratio; W_D , the dissipated energy; W_E , the elastic energy (Kramer, 1996).

Instead, the incremental nonlinear approach consists of the step-by-step integration of the equations of motion, obtained according to a nonlinear constitutive model of the soil. This latter approach has several disadvantages. By way of example, it would not be possible to apply the superposition principle or other tools of the linear analysis, such as, e.g., transfer functions. Furthermore, from a theoretical point of view, the solution of nonlinear differential equations presents greater complexity than linear ones (Kramer, 1996). Even when solving them by means of numerical methods, their solution may present convergence problems and may require several iterations. Therefore, a purely nonlinear approach involves greater complexity of the algorithms and a considerable computational burden. As a result, codes that use this approach are more problematic to build and test. This translates into significant costs. To limit these drawbacks and reduce the computational burden, many simulation codes use a linear equivalent approach (Kramer, 1996). According to this approach, a simulation code, starting from the reference earthquake, provided as an input accelerogram, integrates the equations of dynamic motion, based on initial values for the elastic moduli and damping ratios, to calculate the maximum strain γ_{Max} at every point of the model. From the effective strain values, given by $\gamma_{eff} = \alpha \gamma_{Max}$ (α is a coefficient dependent on the magnitude of the seismic event and variable in the range 0.6-0.7), the updated G and D values are achieved through the curves describing the soil non-linearity of shear modulus and damping ratio. Then, the current G and D estimates are compared with those achieved in the

previous iteration. If both relative differences are less than a desired threshold, the iterations stop, otherwise the calculation is repeated until this condition is satisfied.

The equivalent linear approach significantly reduces the complexity of elastic wave propagation equations and models in heterogeneous media with nonlinear viscoelastic behavior, allowing efficient software to be produced at limited costs and capable of being executed in a reasonable time range.

3.2. Numerical simulation code used in this study

To have a rational balance between the analysis accuracy and the computational burden, able to consider the non-linear behaviour of soil, the local seismic effects, and the geological complexity of middle Aterno River basin, it was decided to resort to the 2D equivalent linear modelling. Based on these considerations, for the AFs evaluation, LSR 2D code by software house Stacec s.r.l. (https://www.stacec.com/lsr-2d_pp92.aspx) was used. LSR 2D performs the 2D equivalent linear modelling by using the finite element approach, in the time domain and in total stresses, and the Kelvin-Voigt model. In the 2D analysis with equivalent linear and concentrated masses approach, the subsoil model is discretized in a mesh with triangular or preferably quadrangular shape elements. Mesh generation is one of the most significant steps of the analysis, depending on it both the accuracy of the solution and the computational burden. It can be said that more the mesh is dense, more the solution is accurate and greater the time and memory required for processing. The use of an excessively coarse mesh results in a filtering of the high frequency components (Fig. 3).

The reason is that nodes too far apart cannot adequately model small wavelengths. Therefore, the height *h* of each element has to be chose following the equation (2).

$$h \leq \left(\frac{1}{8} \div \frac{1}{5}\right) \frac{V_s}{f_{max}} \tag{2}$$

where: *h* is mesh step; *V_s*, the shear wave velocity; *f_{max}*, the maximum frequency considered in the analysis (usually equal to 20-25 Hz).

In this case study, the mesh generation was built with an adaptive approach, so as to preserve computational resources in favor of the control points identified for obtaining the output results. The mesh step would increase from higher values starting from bedrock (equal to 4 m) and then level off at lower values (equal to 1 m), in the proximity of the control points. The overall balance is expressed by the following system of equations (3).

$$M\ddot{u} + C\dot{u} + Ku = -Ma_g \tag{3}$$

where *u* is the vector of nodal displacements; *M*, *K* and *C* refer respectively to the matrix of masses, stiffness and damping; *a_g*, the time history of the acceleration input. The equations (2) are solved by direct integration

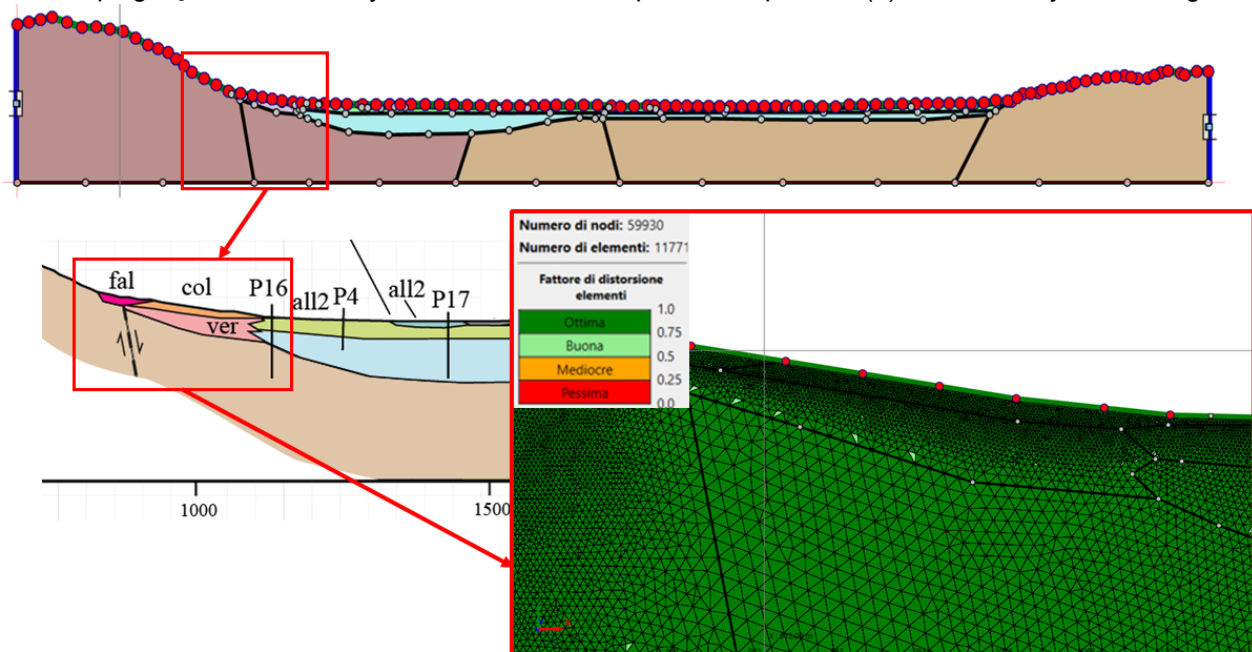


Figure 3. Section A-A' (Preturo-Sassa area): details of the mesh by LSR 2D code.

in the time domain with the Newmark method and with the CAA method (Constant Average Acceleration) which is stable and does not introduce any numerical damping. The seismic motion input a_g is applied simultaneously to the nodes of the bedrock base in the form of P and S waves with a vertical propagation.

The nonlinear soil behavior is taken into account by performing equivalent linear analysis. The dissipative properties of the soil are modeled through the matrix dissipation C . It derives from the assembly of the dissipation matrices of the individual elements calculated according to the complete Rayleigh equation (4).

$$C_i = \alpha_{Ri}M_i + \beta_{Ri}K_i \quad (4)$$

where α_{Ri} and β_{Ri} are the Rayleigh coefficients, C_i is the damping matrix, M_i is the mass matrix and K_i is the stiffness matrix.

The adoption of the Rayleigh equations involves a frequency-dependent damping, which can affect appreciably the modeling results. To reduce this effect LSR 2D uses Rayleigh coefficients calculated according to two natural frequencies of soil deposit, ω_n and ω_m (equations 5 and 6).

$$\alpha_{Ri} = \xi_i \frac{2 \omega_m \omega_n}{\omega_m + \omega_n} \quad (5)$$

$$\beta_{Ri} = \xi_i \frac{2}{\omega_m + \omega_n} \quad (6)$$

where ξ_i is the viscous damping ratio of the i -th element; $\omega_m = \omega_1$, the first natural vibration frequency of soil deposit; $\omega_n = n \omega_1$, where n being the odd integer that approximates by excess the predominant frequency ratio of the seismic input ω_{IN} and frequency ω_1 .

The software LSR 2D requires as input, for each soil the following parameters: (i) the volume weight, (ii) the shear modulus, (iii) the damping at low strain, and (iv) the Poisson's ratio; the G/G_0 vs γ and D vs γ curves; the constant α for the calculation of the characteristic value of the shear deformation starting from the maximum value of γ (t) (typically equal to 0.65).

The code LSPR 2D provides as output: (i) the maximum accelerations on all nodes; (ii) the maximum tangential stresses and strains in each element; (iii) the acceleration time history in the selected nodes (vertical and horizontal components).

4. Geological sections and geophysical & geotechnical soil characterization

Many geological sections were elaborated and 2D simulations were carried out ($n = 15$). The sections were traced to cross most of the SM microzones of the pilot areas and the most significant geological boundaries (fault contacts, alluvial terrace scarps, landslides, anthropic deposits, etc.). Moreover, the sections were located close to the geophysical investigations (above all microtremor measurements and down-hole tests) and boreholes to better constrain the subsoil model. They start and end at least 400 m outside the extremes of the section almost always located in the seismic bedrock, so to minimize in the simulations the edge phenomena due to the lateral dispersion of the seismic energy. Orthogonal sections have also been elaborated for checking with the simulations possible 2D phenomena due to seismic directionality.

The geological units were characterized from a geophysical (V_s , Poisson's coefficient) and geotechnical (density, G/G_0 - γ decay curves and D - γ damping) point of view starting from the numerous seismic site characterization and local seismic response studies performed in the L'Aquila area to which we refer (Amoroso *et al.* 2018; Bordoni *et al.*, 2014; Del Monaco *et al.*, 2013; Di Giulio *et al.*, 2014; Durante *et al.*, 2017; Gaudiosi *et al.*, 2013; Lanzo *et al.*, 2011; Macerola *et al.*, 2019; Mannella *et al.*, 2019; Spadi *et al.*, 2022; Tallini *et al.*, 2020) (Tab. 1; Figs. 4, 5 and 6).

5. Numerical modelling

The Amplification Factors (AF) were calculated with LSR2D code along the sections every 30-50 m and with 3 calculated points located in a zone of 70 m, as a minimum, and 120 m, as a maximum. After the calculation of AFs, a 3-data filtering was performed to make the trend of the AF values homogeneous along the progressives of the section (Figs. 5 and 6). Since 2D simulations have been performed for each microzone, more points are available in which the AFs have been calculated. Therefore, based on an evaluation in favour of safety and subject to expert judgment, the AF of the microzone is the highest of those calculated within the

microzone for the period interval 0.1-0.5 s and the accelerograms and response spectra representative of the microzone refer to those of the AF attributed to it.

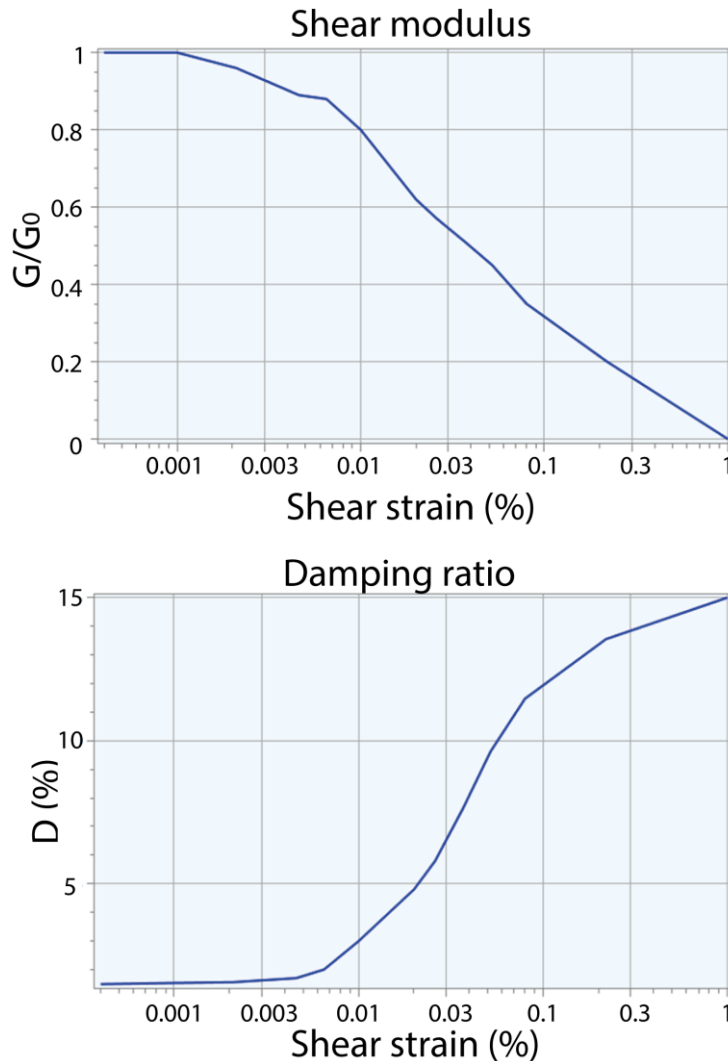


Figure 4. Decay curve G/G_0 - γ (top) and damping curve D - γ (bottom) obtained from resonant column and cyclic torsion test on sample S3 C3 sampled in the borehole S3 at 17.5-18.0 m bgl (Cese Preturo) (MS-AQ Working Group, 2010).

To evaluate the reliability of the calculated AFs, a quality control was performed by comparing the AFs with the geological and the first level SM maps. Indeed, it has been noted that the distribution of the calculated AFs is congruent with the geological background. In fact, along the sections a rough correspondence between the boundaries of the AF classes with the geological units is observed. Further, for the outcropping geological units, the AF values vary within a narrow range. It has been also observed that the AF values are conditioned by the shallower seismic impedance contrast. However, these observations agree with the theory (Kramer, 1996; Lanzo and Silvestri, 1999) and, therefore, lead us to believe that the AFs obtained with the simulations are to be considered reliable. Moreover, considering the good correlation between the AFs and the geology background, the boundaries of the third level SM microzones were areally extended based on the geological unit boundaries, and via expert judgment (Pergalani *et al.*, 2020).

Table 1. Seismostratigraphic characteristics of the units used in all the numerical simulations.

Unit code	Geological unit	Vs (m/s)	γ kN/m ³	ν	G/G ₀ and D versus γ curve
ant	anthropic deposit	250	17	0.2	Rollins et al. (1998) gravel medium.
fra	landslide deposit	300	20	0.4	Rollins et al. (1998) gravel medium.
all3	Fluvial deposit	sand: 250 gravel: 300	19	0.2	sand. Seed et al. (1986) sand (upper lower) gravel: Rollins et al. (1998) gravel medium.
fal	slope deposit	300	20	0.4	Rollins et al. (1998) gravel medium.
col	colluvium	250	19	0.2	Seed et al. (1986) sand (upper lower)
at3	terraced fluvial deposit	400	19	0.2	Rollins et al. (1998) gravel medium.
at2	terraced fluvial deposit	400	19	0.2	Rollins et al. (1998) gravel medium.
dbf	rock avalanche-debris flow	800	20	0.2	Modoni and Gazzellone (2010)
at1	terraced fluvial deposit	500	20	0.2	Rollins et al. (1998) gravel medium.
ver	slope deposit	1200	21	0.2	Elastic linear (damping: 0,5%)
all2	fluvial deposit	450	19	0.2	sample S3 C3 Cese Preturo (Working Group MS-Aq, 2010)
all1	fluvial deposit	800	20	0.2	Rollins et al. (1998) gravel medium.
sandstone UAP	substratum	800	22	0.2	Elastic linear (damping: 0,5%)
carbonate rocks SCZ	substratum	1250	22	0.2	Elastic linear (damping: 0,5%)

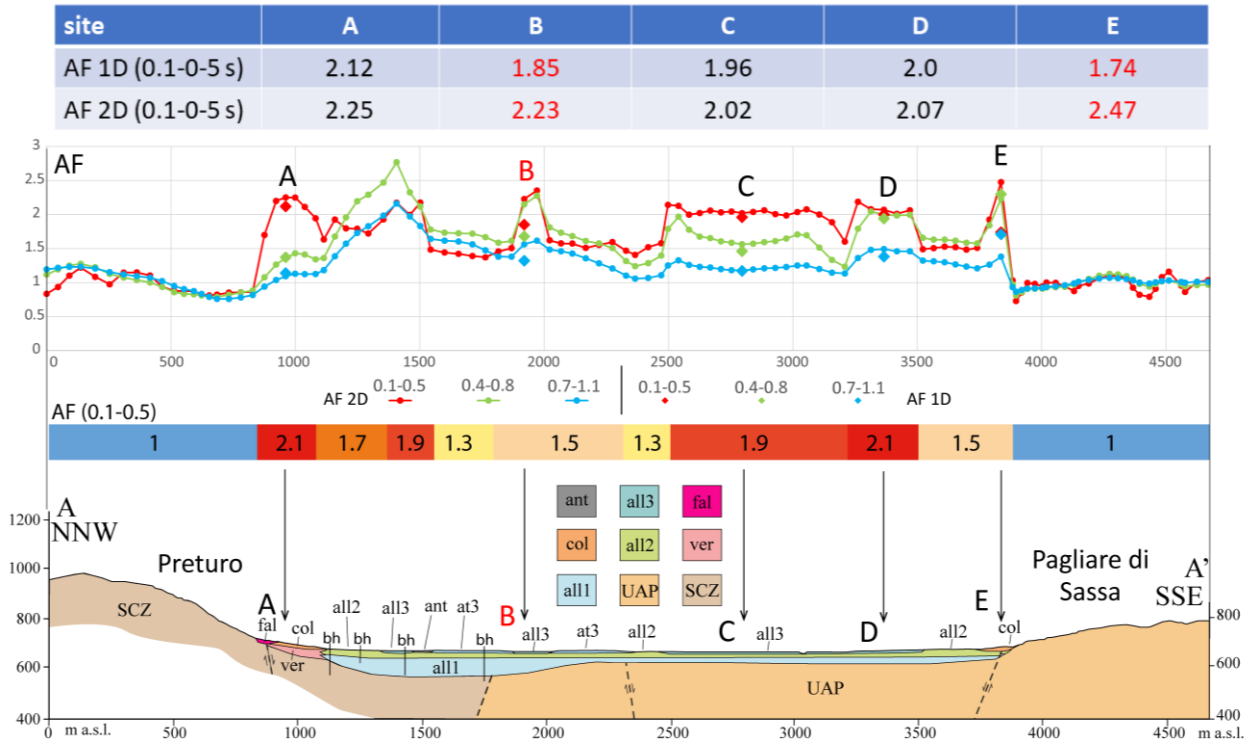


Figure 5. In the Preturo - Pagliare di Sassa area represented in the section A-A' (Fig. 1), a partial 2D basin effect is hypothesized because, in site B located within it, the one-dimensional AF1D (1.85) is lower than the two-dimensional AF2D (2.23). Furthermore, a basin edge effect, as defined in Lanzo and Silvestri (1999), is hypothesized because at site E the AF1D (1.74) is smaller than the AF2D (2.47). The diamond symbol refers to AF calculated with 1D simulation. bh: boreholes; SCZ and UAP: calcareous and terrigenous units belonging to the seismic bedrock; the other units refer to the Plio-Quaternary basin-filling detrital units (see Tab. 1). AF intervals: Class 1.0: $AF < 1.05$; Class 1.1: $1.05 \leq AF < 1.25$ (not present); Class 1.3: $1.25 \leq AF < 1.45$; Class 1.5: $1.45 \leq AF < 1.65$; Class 1.7: $1.65 \leq AF < 1.85$; Class 1.9: $1.85 \leq AF < 2.05$; Class 2.1: $2.05 \leq AF < 2.25$; Class 2.3: $2.25 \leq AF < 2.45$ (not present).

To evaluate the reliability of the calculated AFs, a quality control was performed by comparing the AFs with the geological and the first level SM maps. Indeed, it has been noted that the distribution of the calculated AFs is congruent with the geological background. In fact, along the sections a rough correspondence between the boundaries of the AF classes with the geological units is observed. Further, for the outcropping geological units, the AF values vary within a narrow range. It has been also observed that the AF values are conditioned by the shallower seismic impedance contrast. However, these observations agree with the theory (Kramer, 1996; Lanzo and Silvestri, 1999) and, therefore, lead us to believe that the AFs obtained with the simulations are to be considered reliable. Moreover, considering the good correlation between the AFs and the geology background, the boundaries of the third level SM microzones were areally extended based on the geological unit boundaries, and via expert judgment (Pergalani et al., 2020).

To verify the quality control of the simulations and to refine the local seismic behaviour, any 2D effects were analyzed by comparing the AFs obtained with the 1D simulation with those calculated with the 2D ones in the same site. In several cases, the 2D basin effects were detected, as the AFs calculated in the basin center with 1D modelling was lower than the AFs estimated with 2D one (Fig. 5). Moreover, near the slope break between the reliefs and the Aterno R. plain, the AF values calculated with 2D simulation are higher with respect to those 2D-estimated in the surrounding areas and are lower than those estimated with 1D modelling. This behaviour would probably be attributable to 2D basin edge effect (Lanzo and Silvestri, 1999) (Fig. 5).

For almost all the sections of the Bazzano-Monticchio area crossing the Aterno R. plain, the AF values increase for the intervals of the higher periods, i.e., a shift of the seismic energy towards higher periods is noted (lower frequencies) (Fig. 6). This behaviour seems to be linked to 2D effect because the FAs calculated in points

located on the Aterno R. plain with a 1D modelling are generally lower than the FAs estimated with the 2D one (Kramer, 1996).

Finally, for some microzones not covered by 2D simulations, 1D ones were performed with LSR2D and Strata code (Kottke and Rathje, 2009).

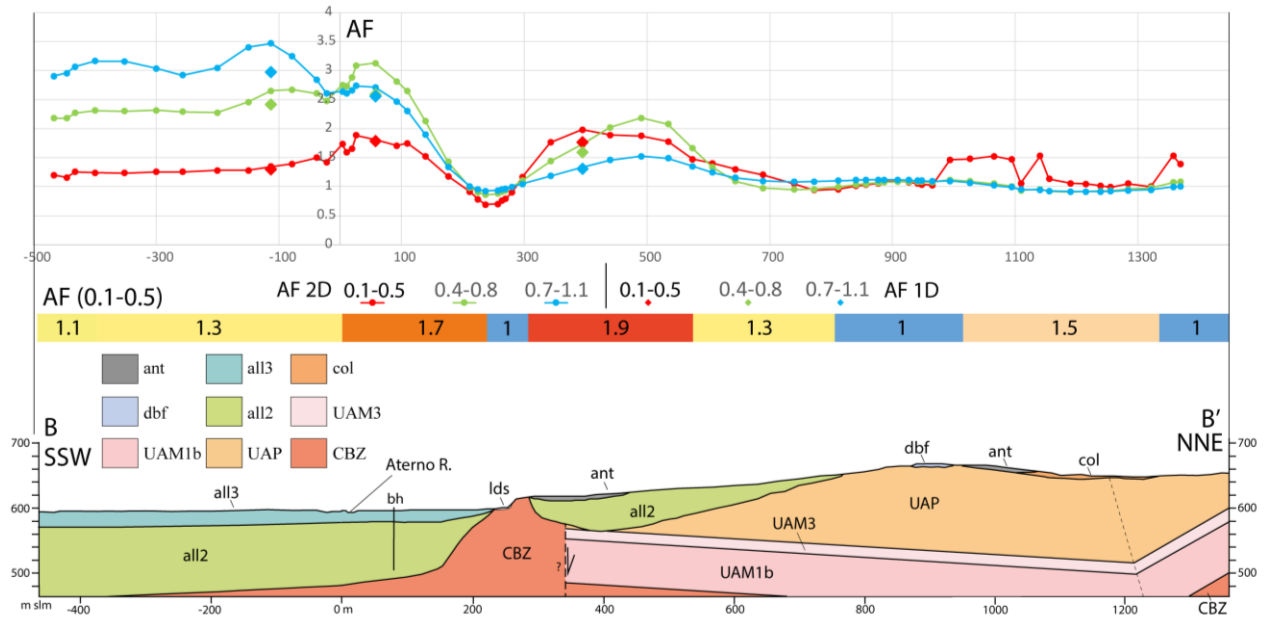


Figure 6. In the Bazzano – Monticchio area represented in the section B-B' (Fig. 1), the AF values increase for the intervals of the higher periods, i.e., a shift of the seismic energy towards higher periods is noted (lower frequencies). The diamond symbol refers to AF calculated with 1D simulation. bh: boreholes; lds: landslide; CBZ and UAM3, UAM1b, UAP: calcareous and terrigenous units belonging to the seismic bedrock; the other units refer to the Plio-Quaternary basin-filling detrital units (see Tab. 1). AF intervals: Class 1.0: $AF < 1.05$; Class 1.1: $1.05 \leq AF < 1.25$; Class 1.3: $1.25 \leq AF < 1.45$; Class 1.5: $1.45 \leq AF < 1.65$; Class 1.7: $1.65 \leq AF < 1.85$; Class 1.9: $1.85 \leq AF < 2.05$.

6. The third level SM deliverables

The following documents have been produced for the Preturo-Sassa and Bazzano-Monticchio areas (L'Aquila Municipality): (i) third level SM maps of the AFs for the three period intervals (0.1-0.5 s, 0.4-0.8 s, 0.7-1.1 s) at 1:5000 scale; (ii) database organized by using the CNR-IGAG plugin "MzS Tools" operating on QGIS ver. 3.22 (Cosentino and Pennica, 2022).

For each microzone, the following data were also produced: (i) n. 3 AFs, one for each period interval (0.1-0.5 s, 0.4-0.8 s, 0.7-1.1 s); (ii) n. 7 natural accelerograms used as seismic input for the 2D modelling; (iii) n. 7 elastic acceleration response spectra at 5% damping (output spectra) at the surface, one for each input accelerogram; (iv) the representative output spectrum of the microzone, i.e., the average spectrum of the 7 above mentioned spectra; (v) the $V_{s,eq}$ value and the related subsoil category according to CS.LL.PP. (2018). The $V_{s,eq}$ value was calculated, for each microzone, using the average thickness of the seismolayers and the relative values of V_s used for the modelling. In Figure 7, as an example, the third level SM map of Preturo is reported for the period interval of 0.1-0.5 s.

7. Conclusions

Considering the complex seismostratigraphy of L'Aquila territory, 2D modeling was carried out on a very large number of sections (n. 15) to calculate in-depth the AFs and analyze their areal variation. The validity of 2D modelling was confirmed by the congruence between the geological background and the AFs value distribution. The nonlinear soil behaviour is taken into account by performing equivalent linear simulations.

The validity of 2D modelling was confirmed by the congruence between the geological background and the AFs value distribution. The 2D modelling allowed to verify the existence of basin and basin edge effects via

- CS.LL.PP. (2018). *Aggiornamento delle Norme tecniche per le costruzioni*. Gazzetta Ufficiale della Repubblica Italiana, 42.
- Cosentino G., Pennica F. (2022). *Manuale d'uso del plugin MzS Tools*. <https://mzs-tools.readthedocs.io/it/latest/intro.html>.
- Del Monaco F., Tallini M., De Rose C., Durante F. (2013). HVNSR survey in historical downtown L'Aquila (central Italy): site resonance properties vs. subsoil model. *Engineering Geology*, 158: 34-47, doi: 10.1016/j.enggeo.2013.03.008.
- Di Giulio G., Gaudiosi I., Cara F., Milana G., Tallini M. (2014). Shear-wave velocity profile and seismic input derived from ambient vibration array measurements: the case study of downtown L'Aquila. *Geophys. J. Int.* (August, 2014) 198 (2): 848-866, doi: 10.1093/gji/ggu162.
- Durante F., Di Giulio G., Tallini M., Milana G., Macerola L. (2017). A multidisciplinary approach to the seismic characterization of a mountain top (Monteluco, central Italy). *Physics and Chemistry of the Earth, Parts A/B/C*, 98: 119-135, doi: 10.1016/j.pce.2016.10.015.
- Gaudiosi I., Del Monaco F., Milana G., Tallini M. (2013). Site effects in the Aterno River Valley (L'Aquila, Italy): comparison between empirical and 2D numerical modeling starting from April 6th 2009 MW 6.3 earthquake. *Bulletin of Earthquake Engineering*, 12(2): 697-716, doi: 10.1007/s10518-013-9540-6.
- Iervolino I., Galasso C., Cosenza E. (2009). REXEL: computer aided record selection for code-based seismic structural analysis. *BEE*, 8: 339-362.
- Kottke A. R., Rathje E. M. (2009). *Technical Manual for Strata*. PEER Report 2008/10, Pacific Earthquake Engineering Research Center, University of California, Berkeley.
- Kramer S. L. (1996). *Geotechnical earthquake engineering*. Pearson Education India.
- Lanzo G., Silvestri F. (1999). *Risposta sismica locale: teoria ed esperienze*. Hevelius Edizioni, Benevento.
- Lanzo G., Tallini M., Milana G., Di Capua G., Del Monaco F., Pagliaroli A., Peppoloni S. (2011). The Aterno Valley strong-motion array: seismic characterization and determination of subsoil model. *Bulletin of Earthquake Engineering*, 9: 1855–1875, doi: 10.1007/s10518-011-9301-3.
- Macerola L., Tallini M., Di Giulio G., Nocentini M., Milana G. (2019). The 1D and 2D seismic modelling of deep Quaternary basin (L'Aquila downtown, central Italy). *Earthquake Spectra*, 35 (4): 1689–1710.
- Mannella A., Macerola L., Martinelli A., Sabino A., Tallini M. (2019). The local seismic response and the effects of the 2016 central Italy earthquake on the buildings of L'Aquila downtown. *Bollettino di Geofisica Teorica ed Applicata*, 60 (2): 263-276, doi: 10.4430/bgta0241.
- Modoni G., Gazzellone A. (2010). Simplified theoretical analysis of the seismic response of artificially compacted gravels. *Proc. V Int. Conf. on Recent Advances in Geotechnical Earthquake Engineering and Soil Dynamics*, San Diego, USA, Paper No. 1.28a.
- MS-AQ Working Group (2010). Seismic microzonation for the reconstruction of L'Aquila. <http://www.protezionecivile.gov.it>.
- Nocentini M., Asti R., Cosentino D., Durante F., Gliozzi E., Macerola L., Tallini M. (2017) - Plio-Quaternary geology of L'Aquila – Scoppito Basin (Central Italy). *Journal of Maps*, 13(2): 563-574, doi: 10.1080/17445647.2017.1340910.
- Nocentini M., Cosentino D., Spadi M., Tallini M. (2018). Plio-Quaternary geology of the Paganica-San Demetrio-Castelnuovo Basin (Central Italy). *Journal of Maps*, 14(2): 411-420, doi: 10.1080/17445647.2018.1481774.
- Pergalani F., Pagliaroli A., Bourdeau C., Compagnoni M., Lenti L., Lualdi M., Madiari C., Martino S., Razzano R., Varone C., Verrubbi V. (2020). Seismic microzoning map: approaches, results and applications after the 2016-2017 Central Italy seismic sequence. *Bulletin of Earthquake Engineering*, 18: 5595-5629.
- Rollins K. M., Evans M. D., Diehl N. B., III W. D. D. (1998). Shear modulus and damping relationships for gravels. *Journal of Geotechnical and Geoenvironmental Engineering*, 124(5): 396-405.
- Seed H. B., Wong R. T., Idriss I. M., Tokimatsu K. (1986). Moduli and damping factors for dynamic analyses of cohesionless soils. *Journal of Geotechnical Engineering*, 112(11): 1016-1032.
- SM Working Group (2008). Guidelines for Seismic Microzonation, Conference of Regions and Autonomous Provinces of Italy – Civil Protection Department, Rome.

- Spadi M., Tallini M., Albano M., Cosentino D., Nocentini M., Saroli M. (2022). New insights on bedrock morphology and local seismic amplification of the Castelnuovo village (L'Aquila Basin, Central Italy). *Engineering Geology*, 297 (2022), 106506, <https://doi.org/10.1016/j.enggeo.2021.106506>.
- Tallini M., Lo Sardo L., Spadi M. (2020). Seismic site characterization of Red Soil and soil-building resonance effects in L'Aquila downtown (central Italy). *Bulletin of Engineering Geology and the Environment*, doi: 10.1007/s10064-020-01795-x.